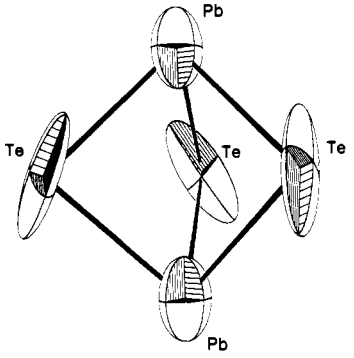

Figure 1. ORTEP view of the $Pb_2Te_3^{2-}$ anion. Ellipsoids are drawn at the 50% probability level.

studies,[3] the $Pb_2Te_3^{2-}$ anion is isostructural with the previously determined $Pb_2Se_3^{2-}$ anion, and their structural differences are in agreement with those proposed.[3] Thus, in the $Pb_2Te_3^{2-}$ anion the Pb-Te distance is 2.943 (2) Å, compared with an average Pb-Se bond length of 2.751 Å in $Pb_2Se_3^{2-}$, while the Te-Pb-Te angles [92.46 (4)° × 6] are significantly larger than the corresponding Se-Pb-Se bond angles [average 89.8 [15]°; range 87.1 (2)-92.4 (1)°] and the Pb-Te-Pb bond angles [67.01 (6)° × 3] correspondingly smaller than the analogous Pb-Se-Pb angles [70.4 (1)-70.9 (1)°]. However, the equatorial Te···Te contacts (4.25 Å) in $Pb_2Te_3^{2-}$ are slightly longer than van der Waals distances (4.12 Å)[7] by amounts very similar to those by which the Se···Se contacts in the $Pb_2Se_3^{2-}$ anion (3.81, 3.89, and 3.95 Å) exceed the Se van der Waals limit (3.8 Å). Finally, the Pb(1)···Pb(1′) distance (3.249 (2) Å) is again significantly less than the approximate van der Waals distances (4.0 Å) but is longer than the corresponding distance in the $Pb_2Se_3^{2-}$ anion (3.184 (3) Å).

Few Pb-Te distances have been reported. Distances of 3.06 and 3.31 Å have been mentioned for the compound $PbBi_4Te_7$,[8] but no values in covalent species are known. The present distances are, however, substantially longer than the Pb(IV)-Te single-bond distance (2.81 Å) and are significantly longer than the Pb(II)-Te single-bond distance (2.86 Å) if the Te covalent radius of 1.32 Å given by Bondi[7] is utilized. However, the Pb-Te distance is in good agreement with the sum of the Te covalent radius (1.37 Å) and the metallic radius of Pb(II) (1.54 Å) of 2.97 Å as given by Pauling.[9] Likewise, the Pb-Se distances in the $Pb_2Se_3^{2-}$ anion correspond resonably well to the sum of the Se covalent radius (1.17 Å) and that of Pb(II) (1.54 Å) to give a value of 2.71 Å. The angle trends between the two anions $Pb_2Se_3^{2-}$, namely, Se-Pb-Se < Te-Pb-Te and Pb-Se-Pb > Pb-Te-Pb, can be rationalized from the electronegativity difference between Se and Te. As one would expect from the VSEPR rules[10] the Ch-Pb-Ch bond angle decreases and the corresponding Pb-Ch-Pb bond angle increases with the more electronegative chalcogen atom. Moreover, as Sanderson[11] has pointed out, the "inert-pair" effect has a substantial effect on electronegativity. Thus, whereas the electronegativities of Ge(IV), Sn(IV), and Pb(IV) are 2.62, 2.30, and 2.29, respectively, those of Ge(II), Sn(II), and Pb(II) are only 0.56, 1.49, and 1.92, respectively. This means that Pb(II) compounds are more polar than corresponding inorganic Pb(IV) compounds. As mentioned in the Introduction, the bond angle trends in the $Pb_2X_3^{2-}$ anions were readily apparent in the relativistically corrected reduced coupling constants $^1K_{RC}$ for these two species in solution.[3] For a fuller discussion of the bonding in the $Pb_2Ch_3^{2-}$ species and their comparisons to related structures, the reader is referred to ref 3, except that we wish to mention here the structural parameters for two other trigonal-bipyramidal molecules, $[(C_6F_5)_2Ge]_3Bi_2$[12] and $(t\text{-BuO})_3Sn^{II}Tl^{I}$,[13] the former because the Bi···Bi separation of 4.005 Å in this compound is normal and considerably longer than that in $Bi_2[W(CO)_5]_3$.[14] However, in the $Sn^{II}Tl^{I}$ species the Sn···Tl separation of 3.306 (3) Å was considered relatively short.

In the (2,2,2-crypt-K^+) moieties, the K···N and K···O distances are 2.75 (2)-2.99 (4) Å.

Acknowledgments. The Natural Sciences and Engineering Research Council of Canada is thanked for providing operating grants (G.J.S.) and an equipment grant for the X-ray diffractometer (Chemistry Department, University of Toronto), and McMaster University and the Ontario Ministry of Colleges and Universities are acknowledged for the award of a fellowship and scholarships, respectively, to M.B.

Supplementary Material Available: Tables of crystal data and refinement results, complete bond lengths and bond angles, and positional parameters for the hydrogen atoms (5 pages); a listing of final structure factor amplitudes (9 pages). Ordering information is given on any current masthead page.

(7) Bondi, A. *J. Phys. Chem.* **1964**, *68*, 441.
(8) Zhukova, T. B.; Zaslavskii, A. I. *Russ. J. Struct. Chem. (Engl. Transl.)* **1970**, *11*, 423.
(9) Pauling, L. *The Nature of the Chemical Bond*, 3rd ed.; Cornell University Press: Ithaca, NY, 1960.
(10) Gillespie, R. J. *Molecular Geometry*; Van Nostrand Reinhold Co.: London, 1972.
(11) Sanderson, R. T. *Inorg. Chem.* **1986**, *25*, 1856.
(12) Bochkarev, M. N.; Razuvaev, G. A.; Zakharov, L. N.; Struchkov, Yu. T. *J. Organomet. Chem.* **1980**, *199*, 205.
(13) Veith, M.; Rosler, R. *Angew. Chem., Int. Ed. Engl.* **1982**, *21*, 858.
(14) Huttner, G.; Weber, U.; Zsolnai, L. *Z. Naturforsh.* **1982**, *37B*, 707.

Contribution from the Department of Applied Science, Brookhaven National Laboratory, Upton, New York 11973

Models of Photosynthetic Chromophores. Molecular Structure of the Bacteriochlorin (2,3,12,13-Tetrahydro-5,10,15,20-tetraphenylporphinato)(pyridine)zinc(II)

K. M. Barkigia,* M. Miura, M. A. Thompson, and J. Fajer*

Received November 27, 1990

Recent X-ray studies of antenna[1] and reaction center[2] bacteriochlorophyll (BChl) proteins have elicited avid experimental and theoretical interest in the physical and chemical properties of bacteriochlorins, both to rationalize photosynthetic light harvesting and energy transduction and to model the efficient and rapid charge separation carried out by photosynthetic organisms.[3] In a different context, the successful use of porphyrin derivatives in phototherapy has prompted a search for chromophores that absorb at longer wavelengths than porphyrins themselves to allow deeper tissue penetration of incident light.[4]

Besides the low structural resolution of the chromophores inherent to BChl proteins,[1,2] few X-ray structures of the generic class of bacteriochlorins exist to guide experimental and theoretical studies. Indeed, only three high-precision structures of bacteriochlorins have been reported to date: a free base[5,6] and a nickel[7]

(1) Tronrud, D. E.; Schmid, M. F.; Matthews, B. W. *J. Mol. Biol.* **1986**, *188*, 443.
(2) Deisenhofer, J.; Michel, H. *Science* **1989**, *245*, 1463. Chang, C. H.; Tiede, D.; Tang, J.; Smith, U.; Norris, J. R.; Schiffer, M. *FEBS Lett.* **1986**, *205*, 82. Yeates, T. O.; Komiya, H.; Chirino, A.; Rees, D. C.; Allen, J. P.; Feher, G. *Proc. Natl. Acad. Sci. U.S.A.* **1988**, *85*, 7993.
(3) For examples, see: *The Photosynthetic Bacterial Reaction Center*; Breton, J., Vermiglio, A., Eds.; Plenum Press: New York, 1988. *Reaction Centers of Photosynthetic Bacteria*; Michel-Beyerle, M. E., Ed.; Springer-Verlag: Berlin, 1990. Hanson, L. K. *Photochem. Photobiol.* **1988**, *47*, 903. Friesner, R. A.; Won, Y. *Biochim. Biophys. Acta* **1989**, *977*, 99.
(4) *Future Directions and Applications in Photodynamic Therapy*; Gomer, C. J., Ed.; Proceedings of SPIE, IS 6; SPIE, Bellingham, WA, 1990.

0020-1669/91/1330-2233$02.50/0

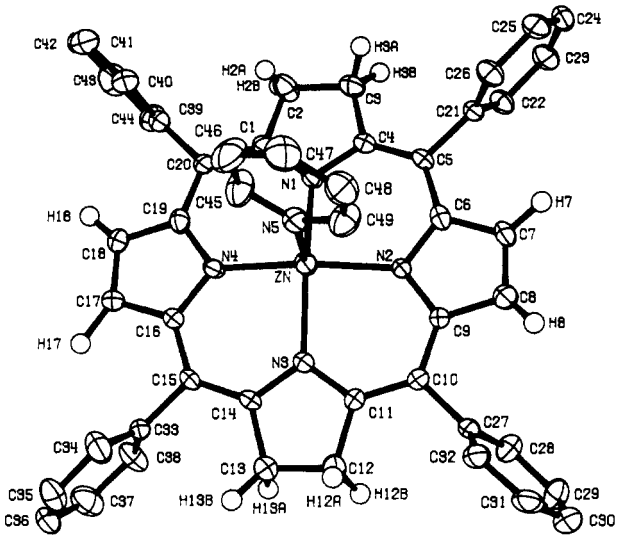

Figure 1. Molecular structure and atom names for ZnTPBC·py. Thermal ellipsoids are drawn to enclose 30% probability. Hydrogens, except those at the β-pyrrole positions, have been omitted for clarity.

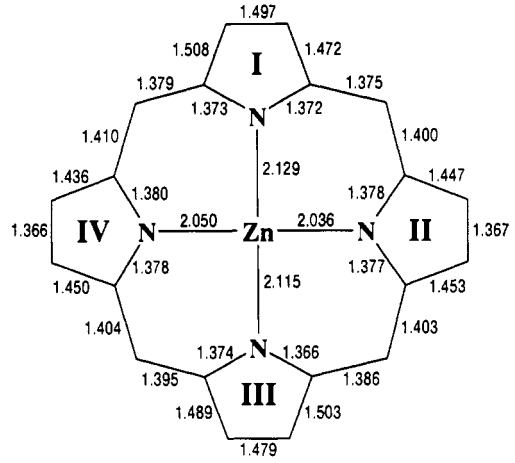

Figure 2. Bond distances (Å) for the core of ZnTPBC. The esd's are 0.004 Å for a typical Zn–N bond and 0.007 Å for a C–C bond.

synthetic derivative and methyl bacteriopheophorbide *a*,[8] derived from the bacteriopheophytin pigment found in reaction centers.[2] We present here an X-ray determination of the bacteriochlorin (2,3,12,13-tetrahydro-5,10,15,20-tetraphenylporphinato)(pyridine)zinc(II) (zinc tetraphenylbacteriochlorin, ZnTPBC). Because the analogous isobacteriochlorin[9] (ZnTPiBC), chlorin[10] (ZnTPC), and (*meso*-tetrapyridyl)porphyrin[11] (ZnTPyP) structures already exist, the present results allow an assessment of the structural consequences of progressively saturating the porphyrin macrocycle. In addition, we use the new structural data to test the validity of the INDO/S semiempirical method[12] in predicting spectral properties of bacteriochlorins. The method has been extensively applied recently to photosynthetic models, antennas, and reaction centers.[3,13]

Table I. Crystal Data for (2,3,12,13-Tetrahydro-5,10,15,20-tetraphenylporphinato)(pyridine)zinc(II)–Pyridine

chem formula: $ZnN_5C_{49}H_{37}\cdot C_5H_5N$	fw = 840.34
a = 11.489 (1) Å	space group: $P\bar{1}$ (No. 2)
b = 13.248 (2) Å	T = 25 °C
c = 14.788 (2) Å	λ = 1.5418 Å
α = 98.92 (1)°	ρ_{calc} = 1.31 g cm^{-3}
β = 94.43 (1)°	μ = 11.26 cm^{-1}
γ = 105.04 (1)°	transm coeff = 0.8584–0.9251
V = 2136.9 Å^3	$R(F_o)$ = 0.060
Z = 2	$R_w(F_o)$ = 0.053

Table II. Final Positional Parameters (×10^4) for the Nonhydrogen Atoms of ZnTPBC

atom	x	y	z
Zn	4299 (1)	1650 (1)	2062 (1)
N1	4370 (4)	74 (3)	1582 (3)
N2	3434 (4)	1635 (3)	804 (3)
N3	4709 (4)	3323 (3)	2310 (3)
N4	5618 (4)	1770 (3)	3121 (3)
C1	4969 (5)	−496 (4)	2051 (4)
C2	4754 (5)	−1608 (5)	1525 (4)
C3	3863 (6)	−1656 (4)	715 (4)
C4	3710 (5)	−580 (4)	799 (4)
C5	2944 (5)	−297 (4)	186 (3)
C6	2837 (5)	728 (5)	182 (4)
C7	2069 (5)	987 (5)	−517 (4)
C8	2258 (5)	2062 (5)	−335 (4)
C9	3089 (5)	2463 (4)	513 (3)
C10	3448 (5)	3522 (4)	971 (3)
C11	4198 (5)	3908 (4)	1800 (3)
C12	4607 (5)	5063 (5)	2230 (4)
C13	5546 (5)	5124 (5)	2995 (4)
C14	5489 (5)	3999 (4)	3032 (3)
C15	6190 (5)	3699 (4)	3699 (3)
C16	6240 (5)	2664 (4)	3748 (3)
C17	7016 (5)	2393 (4)	4438 (4)
C18	6850 (5)	1325 (5)	4209 (4)
C19	5994 (5)	943 (5)	3389 (4)
C20	5665 (5)	−107 (4)	2897 (3)
C21	2142 (5)	−1175 (4)	−552 (4)
C22	2549 (5)	−1540 (4)	−1354 (4)
C23	1784 (6)	−2368 (5)	−1998 (4)
C24	614 (5)	−2848 (4)	−1841 (4)
C25	205 (5)	−2460 (5)	−1053 (4)
C26	958 (5)	−1629 (4)	−401 (4)
C27	2982 (5)	4297 (4)	513 (4)
C28	3400 (5)	4560 (5)	−308 (4)
C29	2943 (6)	5284 (5)	−719 (4)
C30	2100 (6)	5713 (5)	−360 (5)
C31	1690 (6)	5452 (5)	452 (5)
C32	2138 (5)	4776 (4)	905 (4)
C33	7021 (5)	4584 (4)	4406 (4)
C34	6667 (6)	4949 (5)	5224 (4)
C35	7443 (8)	5772 (6)	5857 (4)
C36	8602 (7)	6214 (5)	5710 (5)
C37	8970 (6)	5845 (5)	4930 (5)
C38	8204 (5)	5035 (5)	4248 (4)
C39	6167 (5)	−880 (4)	3332 (4)
C40	5584 (6)	−1396 (5)	3980 (4)
C41	5998 (7)	−2120 (5)	4394 (5)
C42	7036 (7)	−2331 (5)	4138 (5)
C43	7651 (6)	−1856 (6)	3492 (5)
C44	7196 (6)	−1128 (5)	3086 (4)
N5	2689 (4)	1163 (3)	2732 (3)
C45	2726 (6)	754 (6)	3484 (4)
C46	1702 (7)	416 (6)	3927 (5)
C47	592 (6)	468 (6)	3548 (5)
C48	571 (6)	890 (5)	2773 (5)
C49	1602 (6)	1213 (5)	2386 (4)

(5) 3,13-Dimethylene-2,2′,7,8,12,12′,17,18-octaethylporphyrin. Barkigia, K. M.; Fajer, J.; Chang, C. K.; Young, R. *J. Am. Chem. Soc.* **1984**, *106*, 6457.
(6) There are also two reported structures of 2,12-dioxo- and 2,12-dithio-3,3′,7,8,13,13′,17,18-octaethylporphyrins that are formally bacteriochlorins. Arasasingham, R. D.; Balch, A. L.; Olmstead, M. M. *Heterocycles* **1988**, *27*, 2111.
(7) (2,3,12,13-tetrahydro-2′,3′,7,8,12′,13′,17,18-octaethylporphinato)nickel(II) (NiOEBC): Waditschatka, R.; Kratky, C.; Jaun, B.; Heinzer, J.; Eschenmoser, A. *J. Chem. Soc., Chem. Commun.* **1985**, 1604.
(8) MeBPheo. Barkigia, K. M.; Gottfried, D. S.; Boxer, S. G.; Fajer, J. *J. Am. Chem. Soc.* **1989**, *111*, 6444.
(9) Barkigia, K. M.; Fajer, J.; Spaulding, L. D.; Williams, G. J. B. *J. Am. Chem. Soc.* **1981**, *103*, 176.
(10) Spaulding, L. D.; Andrews, L. C.; Williams, G. J. B. *J. Am. Chem. Soc.* **1977**, *99*, 6918.
(11) Collins, D. M.; Hoard, J. L. *J. Am. Chem. Soc.* **1970**, *92*, 3761.
(12) Zerner, M. C.; Loew, G. H.; Kirchner, R. F.; Mueller-Westerhoff, U. T. *J. Am. Chem. Soc.* **1980**, *102*, 589. Ridley, J.; Zerner, M. *Theor. Chim. Acta* **1973**, *32*, 111; 1976, *42*, 223.

Table III. Comparison of Selected Distances (Å) and Angles (deg)

	ZnTPBC	ZnTPC[10,b]	ZnTPiBC[9]	ZnTPyP[11]
C_α–C_β sat	1.493 (8)	1.495 (2)	1.488 (5)	
C_β–C_β sat	1.488 (7)	1.478 (3)	1.489 (5)[a]	
C_α–C_β unsat	1.447 (4)	1.442 (2)	1.444 (2)	1.447 (2)
C_β–C_β unsat	1.367 (7)	1.363 (4)	1.389 (5)	1.355 (4)
Zn–N sat	2.122 (4)	2.130 (1)	2.102 (3)	
Zn–N unsat	2.043 (4)	2.065 (4)	2.070 (3)	2.073 (3)
Zn–N(py)	2.164 (5)	2.171 (2)	2.155 (3)	2.143 (4)
C_α–C_m	1.375–1.410 (7)	1.389–1.416 (2)	1.372–1.419 (3)	1.402–1.413 (4)
C_t–N	2.058	2.054	2.060	2.047
C_t–C_m	3.439	3.445	3.439	3.448
C_t–C_α	3.074	3.070	3.070	3.066
N–Zn–N adj	88.7 (1)	88.6 (2)	88.6 (1)	88.6 (1)
N–Zn–N opp	162.3 (2)	161.6 (1)	162.1 (1)	161.7 (1)
M–N–Cα	125.9 (3)	126.0 (3)	125.8 (4)	126.3 (2)
N–C_α–C_m	125.6 (3)	125.8 (1)	125.9 (2)	125.7 (1)
N–C_α–C_β	110.5 (3)	110.0 (3)	110.3 (4)	109.8 (1)
C_β–C_α–C_m	123.9 (3)	124.1 (3)	123.7 (3)	124.5 (1)
C_α–C_m–C_α	126.4 (4)	125.6 (3)	126.0 (2)	125.2 (3)
C_α–C_β–C_β sat	104.3 (4)	104.3 (2)	104.2 (3)[a]	
C_α–C_β–C_β unsat	106.9 (3)	107.0 (1)	106.3 (2)	106.9 (1)
Cα–N–C_α	108.7 (5)	108.8 (1)	109.0 (3)	
C_α–N–C_α unsat	106.7 (4)	106.8 (2)	106.8 (3)	106.6 (2)

[a] Calculated from ring I only. [b] Recalculated from the coordinates in ref 10.

ZnTPBC[14] crystallizes from py/heptane with a py ligated to the Zn and a py molecule of crystallization. The compound is isomorphous with the corresponding chlorin and isobacteriochlorin, ZnTPC·py and ZnTPiBC·py, respectively.[17] Its molecular structure and atomic nomenclature are shown in Figure 1, crystallographic details are given in Table I, fractional coordinates for the non-hydrogen atoms of the compound are listed in Table II, and bond distances are presented in Figure 2.

All the peripheral hydrogens of the molecule were located in the refinement, and this determination thus establishes the compound as a bacteriochlorin in which the opposing rings I and III are reduced (pyrrolines) and rings II and IV retain the unsaturation of pyrroles. Examination of the bond distances in Figure 2 reveals that the macrocycle possesses pseudomirrors that pass through the N1–Zn–N3 and the N2–Zn–N4 axes such that equivalent bonds in the compound exhibit good internal consistency. As expected for a bacteriochlorin,[8] the average C_α–C_β and C_β–C_β distances of 1.493 (8) and 1.488 (7) Å in the pyrroline rings I and III are longer than the analogous distances of 1.447 (4) and 1.367 (7) Å in pyrrole rings II and IV. They lie within the range of distances found in ZnTPC[10] and ZnTPiBC[9] (Table III), although the mean C_β–C_β bonds in the pyrrolines are shorter than those in MeBPheo[8] and NiOEBC[7] that contain substituents other than hydrogen at the C_β positions. (The possibility has been raised that the shorter distances found in ZnTPC and ZnTPiBC

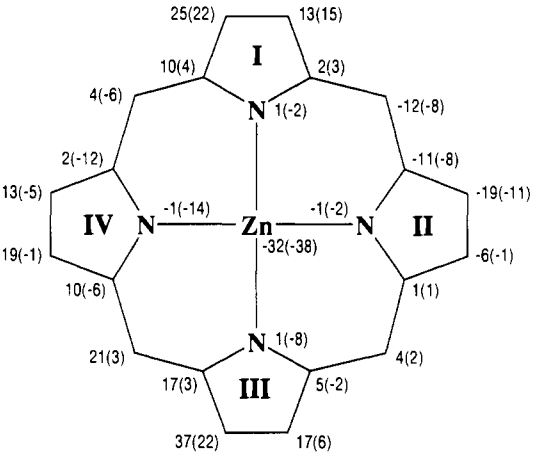

Figure 3. Deviations (in 0.01 Å) from the plane of the four nitrogens and, in parentheses, from the plane of the 24 atoms that comprise the core of the macrocycle.

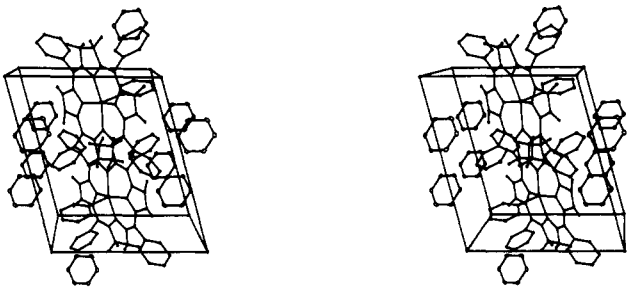

Figure 4. Stereoscopic view of the environment around phenyl ring 3 in ZnTPBC.

are due to rotational disorder[18] or to the refinement model.[19])

The C_α–N–C_α angles open by 2.0° and the C_α–C_β–C_β angles compress by 2.6° in the pyrroline rings, a feature common to hydroporphyrins.[19] The remainder of the angles are relatively unchanged as the macrocycle becomes progressively more saturated in the series P, C, iBC, and BC. Reduction to the bac-

(13) Thompson, M. A.; Zerner, M. C. *J. Am. Chem. Soc.* **1990**, *112*, 7828. Gudowska-Nowak, E.; Newton, M. D.; Fajer, J. *J. Phys. Chem.* **1990**, *94*, 5795. Thompson, M. A.; Zerner, M. C.; Fajer, J. *J. Phys. Chem.* **1990**, *94*, 3820. Scherer, P. O.; Fischer, S. F. *Chem. Phys.* **1989**, *131*, 115.

(14) H_2TPBC was prepared by the method of Whitlock et al.[15,16] Zn was inserted by refluxing the free base with $Zn(OAc)_2$ in dry, degassed pyridine (py) for 24 h under N_2. Crystals of the Zn complex were obtained from py/heptane mixtures at 0 °C. The optical spectra of redissolved crystals in CH_2Cl_2/py (major peaks at 358, 388, 564, 688, and 752 nm) or in CH_2Cl_2 (354, 386, 556, 688, and 752 nm) agreed with previously reported values.[15b,16]

(15) (a) Whitlock, H. W.; Hanauer, R.; Oester, M. Y.; Bower, B. K. *J. Am. Chem. Soc.* **1969**, *91*, 7485. (b) Oester, M. Y. Ph.D. Dissertation, University of Wisconsin, 1971.

(16) Fajer, J.; Borg, D. C.; Forman, A.; Felton, R. H.; Dolphin, D.; Vegh, L. *Proc. Natl. Acad. Sci. U.S.A.* **1974**, *71*, 994.

(17) Unlike ZnTPC and ZnTPiBC, which incorporate a benzene molecule of solvation, the solvate in this study is presumably py, as the compound was crystallized from py/heptane. The structural analysis was thus carried out by assuming a py solvate where the nitrogen is disordered over the six possible ring positions. As a precaution, the analysis was repeated on the assumption that the solvate molecule was benzene; changes in the structural parameters between the two models were insignificant. The data reported here are for the py model.

(18) Scheidt, W. R.; Lee, Y. J. *Struct. Bonding (Berlin)* **1987**, *64*, 1.

(19) Suh, M. P.; Swepston, P. N.; Ibers, J. A. *J. Am. Chem. Soc.* **1984**, *106*, 5164. Strauss, S. H.; Silver, M. E.; Long, K. M.; Thompson, R. G.; Hudgens, R. A.; Spartalian, K.; Ibers, J. A. *J. Am. Chem. Soc.* **1985**, *107*, 4207.

teriochlorin level does not significantly affect the core size. The values of C_t-N, C_t-C_m and C_t-C_α are similar in all four species ($\approx\pm0.01$ Å). The range of C_α-C_m distances (1.375-1.410 (7) Å) does differ from that found in ZnTPyP (1.402-1.413 (4) Å) and is indicative of the differences in π delocalization between the porphyrin and the hydroporphyrins (see Table III).

The Zn-N distances of 2.129 (4) and 2.115 (4) Å in rings I and III are longer than those of 2.036 (4) and 2.050 (4) Å in rings II and IV. Again, this elongation of the M-N (pyrrolines) is common to ZnTPC, ZnTPiBC, and several hydroporphyrins[18,19] and may reflect the wider C_α-N-C_α angles in rings I and III noted above. The M-N (pyrrole) distances are shorter than normally found in pentacoordinated Zn complexes;[18] the reason for the differences is not obvious.

The Zn is displaced 0.38 Å from the plane of the macrocycle toward the axial pyridine and 0.32 Å from the plane of the nitrogens, comparable to the deviations observed for ZnTPC, ZnTPiBC, and ZnTPyP. The Zn-N(py) linkage of 2.164 (5) Å is quite normal[18] and consistent with the values for the rest of the series. The pyridine is situated at 18.1° with respect to the N1-N3 direction and is tilted 6.5° from the normal to the plane of the macrocycle.

The macrocycle exhibits a slight saddle shape (Figure 3) with maximum deviations from the 24-atom plane of 0.22 Å at C2 and C13. Rings I-III are slightly twisted about the C_β-C_β bond with dihedral angles of 3.9, 3.4, and 7.6 (7)°, respectively, while the rotation around C17-C18 is 0.4 (7)°. Phenyl rings 1, 2, and 4 are nearly perpendicular to the macrocycle, but phenyl ring 3 lies at an angle of 69.3°, probably because of interactions with the solvent molecule, which is located 4.88 Å from its center (Figure 4).

Although the molecules pack in pairs, with Zn-Zn distances of 7.48 Å and C_t-C_t distances of 7.09 Å, they are well separated from each other, precluding strong π-π interactions. There are no contacts between adjacent molecules less than 3.9 Å, and the closest approach of ring centers is 4.37 Å between rings I and II in neighboring molecules.

As noted in the introduction, the electronic configurations of BChls are attracting intense theoretical interest because they control the photophysics and photochemistry of the chromophores and, consequently, the primary charge separation in photosynthesis.[3,13] The present results allow a calibration of the INDO/S method commonly used to treat BChls.[13] ZnTPBC offers the advantage of a high degree of symmetry without the complications, common to BChls, that arise from an additional exocyclic ring, orientations of substituents, and diverse deviations from planarity.[13] An INDO/S calculation was thus carried out for ZnTPBC·py, using the crystallographic coordinates reported here, with configuration interactions that included all single-excited configurations from the 10 highest occupied (HOMOs) into the 10 lowest unoccupied molecular orbitals (LUMOs). As expected from previous calculations,[20,21] the near degeneracy of the two HOMOs observed in porphyrins is removed and the HOMO is now a_{1u}, with the difference between the HOMO (a_{1u}) and the HOMO - 1 (a_{2u}) equal to 1.1 eV (for simplicity, the nomenclature associated with the D_{4h} symmetry of porphyrins is retained). EPR results for the cation radical of ZnTPBC that map the unpaired spin distribution of the HOMO support an a_{1u} orbital occupancy.[16] The loss of two double bonds, relative to porphyrins, destabilizes the π system of the bacteriochlorin, and the HOMO rises in energy, in agreement with experimental oxidation potentials: ZnTPBC is easier to oxidize than ZnTPP by $\approx$0.6 V.[16] In contrast to the behavior of the HOMO, the LUMO does not shift appreciably but the LUMO + 1 lies 1.58 eV above, thereby removing the degeneracy of the π^* orbitals found in porphyrins. Again, EPR results support this assignment; the anion radical of ZnTPBC yields well-resolved EPR spectra whereas those of $ZnTPP^{\bullet-}$ are unresolved because of Jahn-Teller effects associated with the degeneracy of the LUMOs.[22] Also, the experimental reduction potentials[16] of ZnTPBC and ZnTPP differ little (<0.1 V), indicating that the LUMOs in porphyrins and bacteriochlorins are nearly isoenergetic.

The invariance of the LUMO and the destabilization of the HOMO in bacteriochlorins result in a much smaller energy gap between the HOMO and LUMO and, consequently, in a significant red shift of the first absorption band of the chromophores relative to porphyrins. In solution, these transitions occur at 602 nm for ZnTPP·py[23] vs 752 nm (13 298 cm^{-1}) for ZnTPBC·py. The INDO calculations for the latter yield a value of 760 nm (13 160 cm^{-1}), a difference of only 8 nm or 140 cm^{-1}. Thus, the method does indeed correctly predict the Q_y optical transitions of bacteriochlorins. Not surprisingly, agreement with higher energy transitions is poorer (as much as 3000 cm^{-1} for the Soret bands), but the calculations clearly provide an adequate electronic description of the chromophores, particularly for the frontier orbitals that are crucial for photochemical activity in photosynthetic electron transfer and photodynamic therapy.

Acknowledgment. This work was supported by the Division of Chemical Sciences, U.S. Department of Energy, under Contract DE-AC02-76CH00016.

Supplementary Material Available: Tables giving complete crystal data, selected bond angles, fractional coordinates for the hydrogen atoms of ZnTPBC, and final positional and anisotropic thermal parameters for the non-hydrogen atoms of ZnTPBC (6 pages); a table of structure factor amplitudes (22 pages). Ordering information is given on any current masthead page.

(20) Gouterman, M. In *The Porphyrins*; Dolphin, D., Ed.; Academic Press: New York, 1978; Vol. III, p 1.
(21) Chang, C. K.; Hanson, L. K.; Richardson, P. F.; Young, R.; Fajer, J. *Proc. Natl. Acad. Sci. U.S.A.* **1981**, *78*, 2652.
(22) Fajer, J.; Davis, M. S. In *The Porphyrins*; Dolphin, D., Ed.; Academic Press: New York, 1979; Vol. IV, p 197.
(23) Nappa, M.; Valentine, J. S. *J. Am. Chem. Soc.* **1978**, *100*, 5074.

Contribution from the Department of Industrial and Engineering Chemistry, Swiss Federal Institute of Technology, ETH-Zentrum, CH-8092 Zürich, Switzerland

Vapor Pressure of Pentacarbonylruthenium, $Ru(CO)_5$

R. Koelliker*,† and G. Bor

Received August 29, 1990

Ruthenium carbonyls play an important role in different catalytic processes with carbon monoxide, e.g., the carbonylation of olefins,[1] the formation of ethylene glycol,[2] the synthesis and homologation of alcohols,[3] and the water gas-shift reaction.[4] The most convenient catalytic precursors for these and other reactions are $Ru_3(CO)_{12}$ and $Ru_4H_4(CO)_{12}$. However, the monomer $Ru(CO)_5$ is readily formed therefrom under reaction conditions upon addition of CO.[5] Despite its importance, the vapor pressure of pentacarbonylruthenium has not been reported until now.

For the investigation of the ruthenium-catalyzed carbonylation of olefins, the thermal carbonylruthenium equilibria between $Ru_3(CO)_{12}$, $Ru(CO)_5$, and CO[6] as well as $Ru_4H_4(CO)_{12}$, $Ru_3(CO)_{12}$, $Ru(CO)_5$, CO, and H_2[6,7] were quantitatively studied in *n*-hexane under elevated temperature and pressure.[5] Therefore, for precise treatment of the data, it is necessary to know the vapor pressure of $Ru(CO)_5$.

$Ru(CO)_5$ is, at room temperature, a colorless liquid that decomposes under light easily to $Ru_3(CO)_{12}$, unless stabilized with CO.[8] To avoid any photochemical reaction, the vapor pressure of $Ru(CO)_5$ has to be determined under the total exclusion of light. At elevated temperature the presence of CO is needed to avoid

† Present address: Department of Organic Chemistry, Weizmann Institute, Rehovot, Israel.

0020-1669/91/1330-2236$02.50/0